Journal of Marine Science and Application (2026) 25: 1238-1251
https://doi.org/10.1007/s11804-025-00782-6

RESEARCH ARTICLE

Double Damage Identification of Fully Free Beams Based on Curvature Modes

Yin Zhang[1], Shengxuan Wei[1], Bihui Pang[1], Haoyue Cheng[1] and Jun Guo[1]

Received: 01 April 2025 / Accepted: 16 June 2025
© Harbin Engineering University and Springer-Verlag GmbH Germany, part of Springer Nature 2026

Abstract

Damage to the ship can threaten its overall strength, which in turn affects the structural safety of the hull and its subsequent use. Recognizing ongoing damage immediately and effectively is crucial. This paper examines a method based on curvature modes to identify ship damage. The effectiveness of this method is investigated when the ship experiences simultaneous and successive damage. The ship is simplified as a hull girder with free boundary conditions. Six different damage cases are analyzed through numerical simulations and experiments. Results show that the curvature mode index can effectively identify two separate damages when the ship is damaged in two locations simultaneously. Additionally, when the ship is subjected to continuous attacks, the curvature mode index can accurately detect new damage without being affected by existing damage. The proposed method offers a novel approach to double damage identification in hull girders, providing valuable insights for real-time ship safety assessment.

Keywords Curvature mode; Hull damage; Double damage identification; Perturbation method; Modal test

1 Introduction

Identifying ongoing damage to ships is crucial for effective damage control and ensuring the safety of lives and property. Ships are often subjected to multiple, successive attacks from different weapons, making it essential to assess the extent of the damage quickly and accurately. Since the start of the Russian–Ukrainian conflict, several warships have been attacked, including the cruiser Moscow. Recently, after Ukrainian drone boats attacked two large Russian patrol ships 340 km southwest of Sevastopol, they also damaged a Russian tank landing ship anchored at the naval base in the port of Novorossiysk, affecting several Russian warships. During these incidents, technicians struggled to assess the loss of hull strength in a timely manner, which notably hampered damage control efforts. The aforementioned case highlights the urgent need for a reliable method to effectively identify ongoing damage in engineering applications.

Only a few effective methods for identifying ship structural damage are currently available, and research on identifying multiple damages to ships is lacking. In this field, Zhang et al. (2022b, 2021a, 2021b, 2020) proposed an indirect damage identification method based on dynamic parameters. This method primarily addresses the problem of stiffness loss. The ship safety assessment focused on the problem of strength loss, and a new method was proposed to calculate strength loss based on stiffness loss. Aiming to address the challenge of assessing ship damage in real time, an indirect damage identification method based on a probabilistic neural network was introduced, which is a data-driven approach. Additionally, an improved damage indicator was defined to locate the damage. In the fields of civil engineering, aeronautical engineering, and bridge engineering, domestic and foreign scholars have made considerable achievements in the identification of multiple damages. With the in-depth research into the damage of large engineering structures, the use of curvature mode shapes to detect multiple damage in beams has become a research focus. However, an inherent limitation of curvature mode shapes lies in their susceptibility to measurement noise, which can diminish their effectiveness in detecting multiple damages. Aiming to overcome this drawback, Cao et al. (2014) investigated the synergy between the wavelet transform and the Teager energy operator to improve the curvature mode shapes. Additionally, Ahmad et al. (2019) used a filtering

Article Highlights

- A double damage identification method based on curvature modes is introduced for double damage identification of beams with free boundary conditions.
- The damage identification method based on dynamic modeling requires less data and is easy to implement in real ship applications.
- This paper provides a technical reference for the practical application of multiple damage identification on ships.

✉ Jun Guo
17798993835@163.com

[1] College of Shipbuilding Engineering, Harbin Engineering University, Harbin 150001, China

technique on curvature mode shapes combined with a gap smoothing method for detecting multiple damages in plate structures, achieving improved results in damage detection. Yang et al. (2012) combined the AWCD method with curvature mode shape data and applied it to the detection of multiple damages in beams. Janeliukstis et al. (2017) developed a damage identification algorithm for beams with multiple damage points based on mode wavelet transform, which effectively captures the damaged regions. Xie et al. (2018) proposed a multidamage identification method for cantilever beams, using modal curvature to locate the damage and employing particle swarm optimization with a Kriging agent model to assess the damage degree. Altunisik et al. (2017) conducted a detailed study on modal parameter identification and vibration-based damage detection for multicracked hollow circular section cantilever beams. Wu et al. (2017) proposed a fast multistage method based on multidamage location assurance criteria and an improved differential evolution algorithm, which successfully identified the exact location and extent of structural damage. Le et al. (2019) introduced a damage identification method for low-density truss core plates, utilizing a flexibility matrix and Teager's energy operator. This method proved to be reliable and effective for identifying single and multiple damages in truss core plates. Hu et al. (2019) simulated the propagation of Lamb waves in steel plates with double cracks and performed damage identification and imaging of double-crack damage in a steel plate. Their approach combined finite element analysis with experimental studies. Kuroki et al. (2011) proposed a method for multiple damage identification and analysis using modified structures, where additional mass is integrated into certain parts of structural members. Ouyang et al. (2016) introduced a method for multiple damage identification and imaging based on an effective Lamb wave response automatic extraction algorithm, which can quickly and efficiently identify single and multiple damages. Ma and Solis (2019) developed a nonmodel-based two-step damage location and quantification method that accurately locates and quantifies multiple closely spaced cracks in a beam. The above studies provide valuable insights and references for research on multiple damage identification in ship structures.

In this paper, the curvature mode method is used to identify double damage in hull girders under various conditions. The modal data are obtained using the finite element method and experimental modal analysis. The total vibration modes of variable-section beams and homogeneous beams are similar; thus, the variable-section hull girders are simplified to homogeneous beams for modeling convenience. The effectiveness of the hull girder damage identification under different conditions is verified through experiments. Using the modal assurance criterion (MAC) method, the measurement point of the acceleration sensor is optimized. Modal shapes of fully free beams in intact, single-damaged, and double-damaged states are obtained through modal tests using the single excitation method. The curvature mode difference and its mean value index are adopted for damage identification of the hull girder. The accuracy of identifying different double damage conditions is analyzed. Under two scenarios of ship attacks, the curvature mode method is demonstrated to be effective for double damage identification, offering a novel approach and methodology for multiple damage identification in ships.

2 Damage identification theory

Ship damage leads to changes in the natural frequency and mode shape of the structure, with mode shapes being more sensitive indicators of damage than frequency shifts. Common modal-based damage identification methods include the MAC, coordinate modal assurance criterion (COMAC), displacement modes, curvature modes, and strain modes. Although higher-order modes are more responsive to local damage, they are challenging to measure accurately and often result in higher recognition errors when using MAC and COMAC. In contrast, the curvature mode method offers superior accuracy in damage detection. Therefore, this study adopts the curvature mode method to identify various double damage scenarios in hull girders.

2.1 Damage localization based on curvature mode

According to the mechanics of materials, the basic formula for one-dimensional beam bending deformation is given as follows:

$$\frac{M(x)}{E(x)I(x)} = \frac{1}{\rho(x)} \tag{1}$$

When a structure is damaged, its bending stiffness decreases, leading to an increase in curvature. Therefore, the curvature mode shape exhibits a notable change. Structural damage can then be identified by comparing the curvature mode shapes before and after damage occurs. According to Pandey et al. (1991), curvature mode shapes can be derived by performing a numerical differentiation of the measured displacement mode shapes.

$$\varphi_i''(x) = \frac{\varphi_i(j-1) - 2\varphi_i(j) + \varphi_i(j+1)}{h^2} \tag{2}$$

where $\varphi_i(j)$ is the ith mode shape value of the jth node, and h is the distance between nodes. Compared with the curvature mode, the curvature mode difference demonstrates a superior capability to discriminate structural damage. Therefore, the curvature mode difference is chosen as the index for damage identification in this paper. The absolute value expression of the curvature mode difference is presented below.

$$\Delta\varphi'' = \left|\varphi_d'' - \varphi_r''\right| \tag{3}$$

where $\Delta\varphi''$ is the curvature mode difference, φ_d'' is the curvature mode of the damaged structure, and φ_r'' is the curvature mode of the intact structure.

A large curvature mode difference typically corresponds to the location of structural damage. By flexibly comparing index changes at each location, damage can be identified with high accuracy. However, in practice, peak values of the curvature mode difference may appear not only near the damage site but also in areas far from the damage, potentially leading to misjudgment. Aiming to eliminate errors associated with higher-order indicators, the average value of the curvature mode difference from the first four mode shapes is used to realize damage localization.

2.2 Damage degree identification based on perturbation method

Based on the Euler–Bernoulli equation, the vibration differential equation of the hull girder is given as follows:

$$\frac{\partial^2}{\partial x^2}\left\{EI(x)\frac{\partial^2\left[v(x,t)\right]}{\partial x^2}\right\} + \rho(x)\frac{\partial^2}{\partial t^2}\left[v(x,t)\right] = 0 \tag{4}$$

where $EI(x)$ is the bending stiffness, $v(x,t)$ is the longitudinal displacement, and $\rho(x)$ is the density of the hull girder per unit length.

Only the local stiffness loss is considered in this study for structural damage simulation, overlooking the mass loss. The separation variable method is adopted to solve the following vibration differential equation:

$$\frac{\partial^2}{\partial x^2}\left\{EI_d(x)\frac{\partial^2\left[\phi_i^d(x)\right]}{\partial x^2}\right\} - \rho(x)\lambda_i^d\left[\phi_i^d(x)\right] = 0 \tag{5}$$

where λ_i^d is the characteristic value of the damaged beam equation, $\phi_i^d(x)$ is the characteristic vector of the solution of the damaged beam equation, $EI_d(x)$ is the damage stiffness. The relationship between the stiffness of intact hull girder is as follows:

$$EI_d(x) = EI_i(x)\left\{1 - \varepsilon\left[H\left(x - x_1\right) - H\left(x - x_2\right)\right]\right\} \tag{6}$$

where $EI_i(x)$ is the stiffness of the intact hull girder, ε is the degree of damage $(0 < \varepsilon < 1)$ for a small amount, $H\left(x - x_i\right)$ is the unit step function, x_1 and x_2 are the starting point and end point of the damaged area.

The smaller ε is expanded using the perturbation method, and the asymptotic solution is as follows (Zhang et al., 2022b).

$$\begin{aligned}\lambda_i^d &= \lambda_i^0 - \varepsilon\lambda_i^1 + o(\varepsilon^2)\\ \phi_i^d(x) &= \phi_i^0(x) - \varepsilon\phi_i^1(x) + o(\varepsilon^2)\end{aligned} \tag{7}$$

The governing equation of a damaged hull girder is derived by substituting the relevant parameters into the differential equation of the vibrating hull girder

$$\varepsilon^0: EI_i\frac{\partial^4}{\partial x^4}\left[\phi_i^0(x)\right] - \lambda_i^0\rho\phi_i^0(x) = 0 \tag{8}$$

$$\begin{aligned}\varepsilon^1: EI_i\frac{\partial^4}{\partial x^4}\left[\phi_i^1(x)\right] - \lambda_i^0\rho\phi_i^1(x) = &-EI_i\frac{\partial^2}{\partial x^2}\\ &\left\{\left[H\left(x - x_1\right) - H\left(x - x_2\right)\right]\frac{\partial^2}{\partial x^2}\left[\phi_i^0(x)\right]\right\} + \lambda_i^1\rho\phi_i^0(x)\end{aligned} \tag{9}$$

The modal shape of the damaged hull girder is shown below.

$$\begin{aligned}\phi_i^d(x) &= \phi_i^0(x) - \varepsilon\phi_i^1(x) =\\ &\phi_i^0(x) - \varepsilon\left\{\sum_{j=1,j\neq i}^{n}\frac{\lambda_i^0}{\lambda_i^0 - \lambda_j^0}\left(G_{1j} - G_{2j} + G_{3j} - G_{4j} - G_{5j}\right)\right.\\ &\phi_j^0(x) + \left\langle x - x_1\right\rangle\frac{\partial}{\partial x}\phi_i^0(x)\Big|_{x=x_1} - \left\langle x - x_2\right\rangle\\ &\left.\frac{\partial}{\partial x}\phi_i^0(x)\Big|_{x=x_2} - \left[H\left(x - x_1\right) - H\left(x - x_2\right)\right]\phi_i^0(x)\right\}\end{aligned} \tag{10}$$

When the hull structure is damaged, the curvature mode difference is calculated, from which the degree of damage is then determined.

$$\begin{aligned}\varepsilon = -\Delta/&\left\{\sum_{j=1,j\neq i}^{n}\frac{\lambda_i^0}{\lambda_i^0 - \lambda_j^0}\left(G_{1j} - G_{2j} + G_{3j} - G_{4j} - G_{5j}\right)\right.\\ &\left.\left[\phi_j^0(x)\right]'' - \left[H\left(x - x_1\right) - H\left(x - x_2\right)\right]\left[\phi_i^0(x)\right]''\right\}\end{aligned} \tag{11}$$

where Δ is the modal difference of hull girder curvature,

$$\begin{aligned}G_{1j} &= \frac{\partial}{\partial x}\phi_i^0(x)|_{x=x_1}\int_0^L\left\langle x - x_1\right\rangle\phi_j^0(x)\,\mathrm{d}x\\ G_{2j} &= \frac{\partial}{\partial x}\phi_i^0(x)|_{x=x_2}\int_0^L\left\langle x - x_2\right\rangle\phi_j^0(x)\,\mathrm{d}x\\ G_{3j} &= \phi_i^0(x_1)\int_0^L H\left(x - x_1\right)\phi_j^0(x)\,\mathrm{d}x\\ G_{4j} &= \phi_i^0(x_2)\int_0^L H\left(x - x_2\right)\phi_j^0(x)\,\mathrm{d}x\end{aligned}$$

2.3 Sensor optimal placement method

For large structures, damage identification typically requires a substantial number of sensors. However, an excessive number of sensor networks raise maintenance costs, funding requirements, and data volume. In addition, during modal testing, the number and placement of sensors notably impact the accuracy of the modal test results,

which, in turn, directly affects the reliability of damage identification. In this paper, the MAC method is selected as an evaluation index to optimize the testing scheme for feature signals. The MAC is calculated as follows.

$$\mathrm{MAC}_{ij} = \frac{\left[\left(\varphi_i^u\right)^{\mathrm{T}}\varphi_j^d\right]^2}{\left[\left(\varphi_i^u\right)^{\mathrm{T}}\varphi_i^u\right]\left[\left(\varphi_j^u\right)^{\mathrm{T}}\varphi_j^u\right]} \tag{12}$$

where $\{\phi_i\}$ and $\{\phi_j\}$ represent mode vectors of orders i and order j, respectively. When the nondiagonal elements of the MAC matrix are equal to 0, it indicates that the i-order and j-order modal vectors are orthogonal and can be easily identified. Conversely, when the nondiagonal element is equal to 1, it means that the intersection angle between the i-order and j-order modal vectors is zero, making the two vectors indistinguishable.

3 Damage simulation

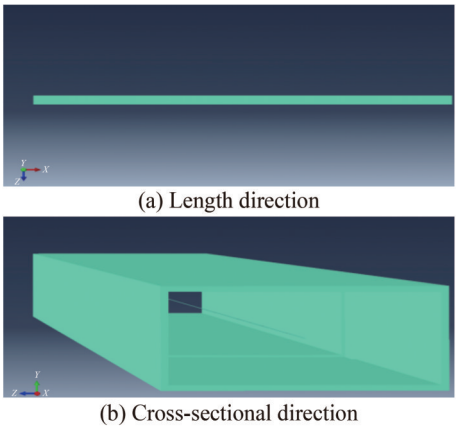
3.1 Finite element model

Two cases of hull girder damage are considered. In the first case, the ship experiences two simultaneous attacks. In the second case, the ship sustains an initial damage and is subsequently subjected to another attack, causing additional damage. A total of six working conditions are defined across the two cases. In working conditions ①, ② and ③, the damage occurs at units 5 and 9, with the same damage degree. In working conditions ④, ⑤ and ⑥, the damage occurs at units 12 and 15, with different damage degrees (shown in Table 1).

The numerical simulation model has dimensions of 6 m in length, 0.2 m in width and 0.1 m in height. Using line modeling applied to the section properties, the model comprises 20 segments and 21 nodes, with each segment measuring 0.3 m in length. The cross-sectional shape is rectangular, and the plate thickness is 5.5 mm, as shown in Figure 1. The material properties are as follows: modulus of elasticity of 2.06×10^{11} Pa, density of 7 850 kg/m^3, and Poisson's ratio of 0.3. The model is subjected to fully free boundary conditions.

Table 1 Damage conditions

Damage condition	Damage unit	Degree of damage		
Based on the intact condition	Unit 5	15%	25%	45%
	Unit 9	15%	25%	45%
	Working condition	①	②	③
	Unit 12	25%	45%	15%
	Unit 15	15%	25%	45%
	Working condition	④	⑤	⑥
Based on single damage condition	Unit 5	15%	25%	45%
	Unit 9	Pre-existing damage		
	Working condition	③	④	③
	Unit 12	25%	45%	15%
	Unit 15	Pre-existing damage		
	Working condition	⑤	⑥	⑦



(a) Length direction

(b) Cross-sectional direction

Figure 1 Simulation model

According to the vibration equation of the hull girder, the vibration modes are determined based on the modal displacements in the vertical degrees of freedom at the 21 nodes. Aiming to stimulate stiffness loss, different section sizes are assigned by varying the plate thickness, thereby reducing the sectional moment of inertia. The plate thickness values corresponding to different damage degrees are listed in Table 2. Modal analysis of the simulation model to extract vibration pattern data under intact and damaged conditions across various working scenarios.

Table 2 Damage degree corresponds to the thickness of the section plate

Section plate thickness (mm)	Degree of damage
5.5	intact
4.6	15%
4.0	25%
2.8	45%

3.2 Experimental model

The dimensions of the experimental model are similar to those of the FE model, with a total weight of 169.96 kg and a material density of 7 850 kg/m^3. The model comprises 20 segments and 21 nodes, as shown in Figures 2 and 3, respectively. The experimental model is divided into three groups. The first group represents the beam in its intact condition. The second group corresponds to the beam with single damage, and the third group includes the beam with

double damage. The damage conditions are similar to those in the simulation, divided into two cases with six damage conditions. During the damage tests, stiffness loss is simulated by introducing notches of different sizes to the corresponding elements, as shown in Figure 4.



Figure 2 Experimental model

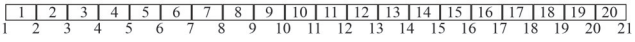


Figure 3 Node numbers

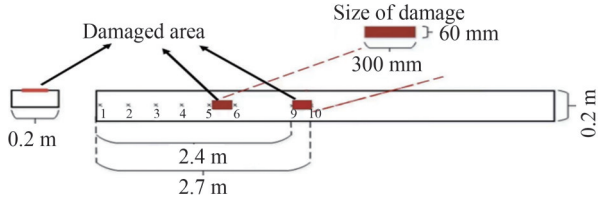


Figure 4 Stiffness loss simulation diagram

The notch sizes corresponding to damage units with different damage degrees are shown in Table 3.

Table 3 Notch size and stiffness loss

Damage simulation	Schematic	Notch size	Stiffness loss
Notch 1		300 mm × 60 mm	15%
Notch 2		300 mm × 96 mm	25%
Notch 3		300 mm × 146 mm	45%

The structure is often supported using suspension bracing and fixed bracing to simulate free boundary conditions. Suspension bracing involves suspending the structure with elastic ropes, allowing it to move freely within a fixed space. This type of support minimally influences the behavior of the beam model. In addition, to further improve the accuracy of boundary condition simulation, the positions of the suspension points are determined based on the modal characteristics of the test model. The effects of the limitations of experimental conditions are effectively reduced by placing the suspension points at nodes corresponding to higher-order vibration modes.

The Donghua5902 modal test system is used in the experiment. This system comprises a data acquisition instrument, a laptop computer equipped with embedded modal analysis software, and a force hammer, as shown in Figure 5. Based on the modal characteristics of the model, 13 acceleration sensors are employed to conduct the modal tests.

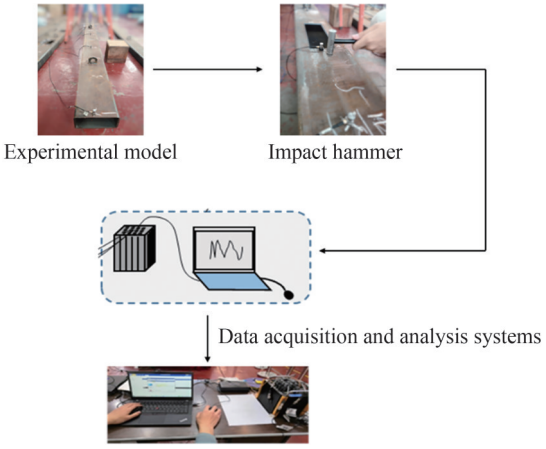


Figure 5 Test design diagram

The single-input–multi-output method is used to identify and analyze the modal information of the test model. Aiming to minimize errors in calculating the frequency response function from a single test, the dynamic response signal (Figure 6) is recorded using five excitations. The corresponding frequency response information is then linearly averaged to reduce experimental errors and improve accuracy.

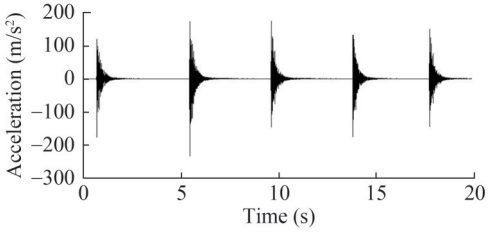


Figure 6 Dynamic response signals

3.3 Sensor placement optimization and verification

According to the sensor placement optimization method based on the MAC, the optimal placement of measurement points should minimize the nondiagonal elements of the MAC matrix. In this study, the sum of all elements in the MAC matrix is used as the evaluation index. The placement

scheme of the measurement points is determined through iteration, aiming to minimize this index.

The basic principle of sensor placement is to avoid positioning sensors at the nodes of vibration modes and, as much as possible, to arrange them at the amplitude points of the vibration mode. Aiming to improve the accuracy of mode shape identification, all amplitude points are taken as measurement points in this study. The test object in this paper is an equivalent beam. Aiming to effectively capture modal information during testing, predictive research on the modal information of the test model is required. Therefore, in this paper, the finite element method is used to conduct a preliminary modal analysis, identifying the modes of the test model and obtaining node information of different orders. The vibration modes are shown in Figure 7, and the corresponding location information of amplitude points and nodes is shown in Table 4.

According to Table 4, nodes 3, 6, 8, 14, 16, and 19, identified as modal nodes rather than amplitude points, are excluded to improve the accuracy of vibration mode identification. Based on the amplitude points of each order mode and the measuring points in the beam, the initial measuring point scheme includes the following nodes: 1, 4, 5, 7, 9, 10, 11, 12, 13, 15, 17, 18, and 21. Aiming to account for potential sensor misalignment, adjacent nodes to these initial measuring points are regarded as alternative measuring points. The complete set of available measurement point options is as follows: 1 (2), (3) 4, 5 (6), 7 (8), 9, 10, 11, 12, 13 (14), 15 (16), 17, 18 (19), (20) 21, where the nodes in parentheses represent the alternative measurement points. By arranging and combining these options, 256 kinds of test point schemes can be obtained. An algorithm was developed to evaluate these configurations, and the optimal measurement point scheme was obtained, as shown in Table 5. Additionally, four sets of verification point schemes were included to assess the effectiveness of the selected configuration. Aiming to minimize errors in the frequency response function during a single test, each dynamic response signal was recorded over five excitations and then averaged linearly.

Notably, the table shows that the evaluation index value of the optimal test scheme is the lowest. This finding indicates that the vibration modes obtained using this scheme exhibit good orthogonality and meet theoretical require-

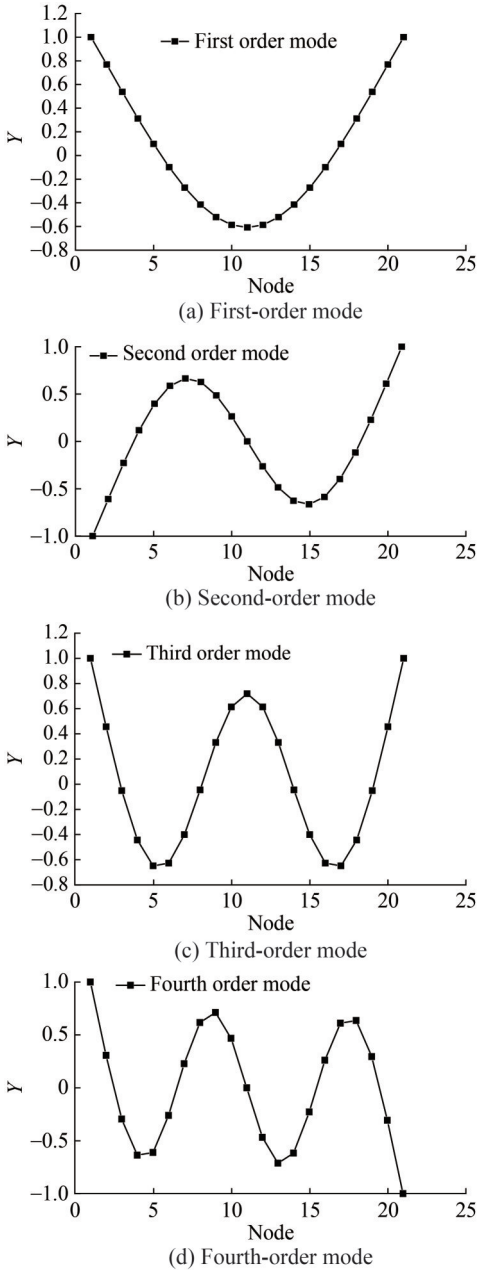


Figure 7 Finite element mode shapes

Table 4 Amplitude point and node location information

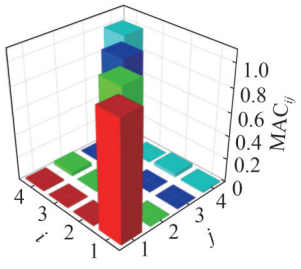
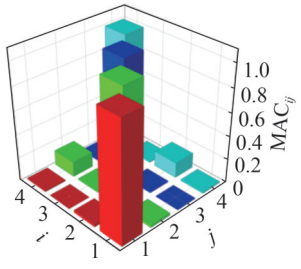
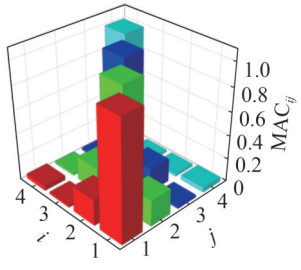
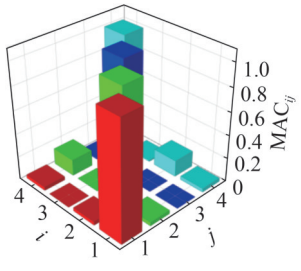
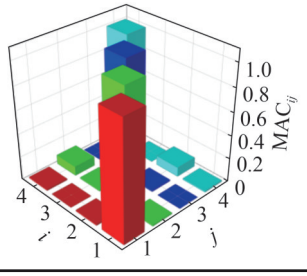
1st order		2nd order		3rd order		4th order	
Amplitude point	Node	Amplitude point	Node	Amplitude point	Node	Amplitude point	Node
1	6	1	4	1	3	1	3
11	16	7	11	5	8	4	7
21		15	18	11	14	9	11
		21		17	19	13	15
				21		18	19
						21	

ments. Therefore, the effectiveness of the test scheme evaluation method proposed in this paper is verified.

4 Discussion of results

Modal analysis is performed on the finite element model and the test model to obtain their respective vibration modes. Based on two conditions, intact damage and single damage, a self-programmed algorithm using the curvature mode difference is applied for damage identification. The study investigates the effectiveness of the curvature mode-based method in cases where two damages occur simultaneously or when additional damage is sustained after initial damage has already occurred.

Table 5 Model testing scheme index values

Scheme	MAC diagram	Measure point	Evaluation index
Optimal		1, 4, 6, 8, 9, 10, 11, 12, 14, 15, 17, 18, 21	4.08
Verification 1		1, 3, 5, 7, 9, 10, 11, 12, 13, 16, 17, 19, 21	4.36
Verification 2		2, 3, 5, 8, 9, 10, 11, 12, 13, 15, 17, 19, 20	5.04
Verification 3		2, 4, 6, 7, 9, 10, 11, 12, 14, 16, 17, 18, 20	4.42
Verification 4		1, 4, 5, 8, 9, 10, 11, 12, 14, 15, 17, 18, 21	4.22

4.1 Damage identification based on intact condition

The maximum value of the curvature mode difference should correspond to the location of the damage. When the ship suffers two simultaneous damage events, the identification results obtained from the FM models using the curvature mode difference are shown below.

Figure 8 shows that the overall curvature modes difference for each order is the largest at units 5 and 9. Among the results, the 3rd- and 4th-order curvature mode differences accurately identify the two damage locations. Moreover, the magnitudes of these value at the two damage units are remarkably similar, which is consistent with that the two damage units have the same degree of damage. The 2nd-order curvature mode difference identifies only one damage at unit 5, while the 1st- order curvature mode difference identifies only unit 9 as the damaged unit. As the order of the curvature mode difference increases, the peak value of this index also gradually increases. For working condition ④, the overall trend of the curvature mode difference for each order shows the largest peak near unit 12. According to the 3rd- order curvature mode difference, the damage is also observed in unit 15; however, the damage degree at unit 12 is more severe. This finding is consistent with 2nd- and 4th-order curvature mode differences, which are not pronounced at unit 15. The 1st order curvature mode difference identifies only unit 12 as damaged. For working condition ⑤, the results are similar to those of working condition ④, corresponding to the actual situation where unit 12 is more damaged than unit 15. In working condition ⑥, the curvature mode difference peaks of all orders are largest near unit 15, reflecting that unit 15 is more severely damaged than unit 12, revealing notable differences in damage degree. In this case, the curvature mode differences at all orders only identify unit 15 as damaged.

The curvature mode differences of the first four orders are averaged, and the working conditions with the same damage unit but different damage degrees are compared. The results are shown in Figure 9.

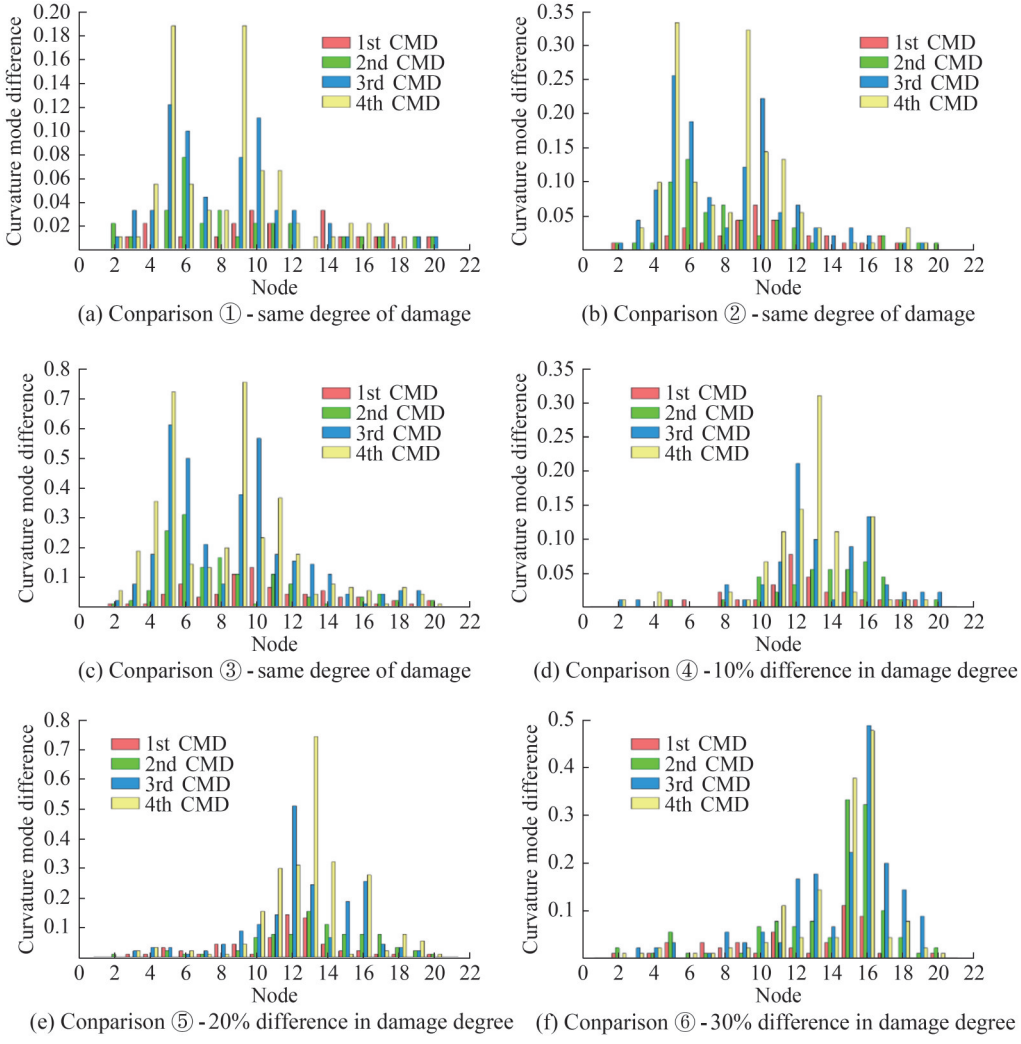


Figure 8 Simulation curvature mode difference for two simultaneous damage

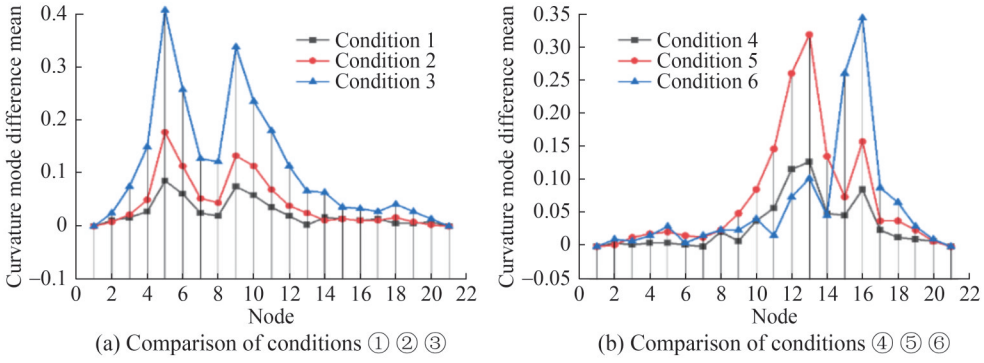


Figure 9 Average of the curvature mode difference of simulation results for two simultaneous damage

The simulation results shown in Figure 9 indicate that the peaks in the average curvature mode differences for the first four modes correspond accurately to the two damage locations in the hull structure. For working conditions ①, ②, and ③, where the damage degree is the same at both locations, the peak values of the index are similar at these damage locations. With the increase in the damage degree of the unit, the index at the corresponding damage location gradually increases, demonstrating a clear differentiation. For working conditions ④, ⑤, and ⑥, the damage degree differs between the two locations. Specifically, in conditions ④ and ⑤, the damage at unit 12 is greater than that at unit 15, whereas in working condition ⑥, the damage at unit 15 exceeds that at unit 12, exhibiting the largest difference in damage.

The experimental results of double damage identification using the curvature mode difference in the intact condition are shown below.

Figure 10 shows that for conditions ①, ②, and ③, the curvature mode difference generally exhibits the highest values near units 5 and 9. In conditions ① and ②, some interference peaks exist in the 2nd- and 4th-order curvature mode differences, while the 3rd-order curvature mode difference accurately identifies the two damaged units. As the damage degree increases, as in condition ③, the interference peaks in all orders of curvature mode difference gradually diminish, allowing for highly accurate localization at units 5 and 9. For condition ④, the peak value of the 1st-order curvature mode difference is highest at units 12 and 15. The 2nd-order peak is located at unit 15, while the 3rd- and 4th-order peaks are largest at unit 12, although interference peaks are present. In condition ⑤, the 1st and 2nd-order curvature mode differences peak at unit 12, whereas the 3rd- and 4th-order curvature mode differences more accurately identify units 12 and unit 15. For condition ⑥, the curvature mode differences of all orders are largest at unit 15, which corresponds to the substantial difference in damage degree between units 15 and 12.

The mean values of the curvature mode differences for different damage degrees in the experiment are compared, with the results presented in Figure 11.

The peak values of the curvature mode differences across the first four modes correspond to the two damaged units in all six working conditions. Conditions ①, ② and ③ are identified in unit 5 and 9. Conditions ④, ⑤ and ⑥ are identified in unit 12 and 15. The identification results are accurate. The degree of damage is positively correlated with the peak value and the differentiation is obvious.

When the ship sustains two simultaneous damages, the mean curvature mode difference index can accurately identify both damaged units. This index is positively correlated with the damage degree, and the mean values corresponding to two elements with the same damage degree are notably similar. Therefore, the damage degree can be assessed based on the magnitude of changes in the curvature mode difference. In comparison, the experimental results show varying levels of interference peaks, which are attributed to noise interference and changes in vibration modes caused by the suspension position. However, compared to previous studies (Cheng et al., 2023), these interference peaks have been substantially reduced, demonstrating the effectiveness of the sensor optimization method.

4.2 Damage identification based on single damage condition

When the hull sustains additional damage on top of an existing one, the results from the finite element model using the curvature mode difference are presented below.

When the existing damaged unit is unit 9, the overall trend of the curvature mode difference for conditions ①, ② and ③ is the largest in unit 5. It is consistent with the actual damage unit. When the damage degree is relatively small, as in condition ①, the 1st order curvature mode difference is identified in unit 5 and 10. With the increase of the order, the peak value of curvature mode difference gradually increases. When the existing damaged unit is 15, the overall trend of curvature mode difference for conditions ④, ⑤ and ⑥ is the largest in unit 12, which accords with the actual damaged area. The damage degree of unit 12 under condition ⑥ is less than that under condition ④ and less than that under condition ⑤. When the damage

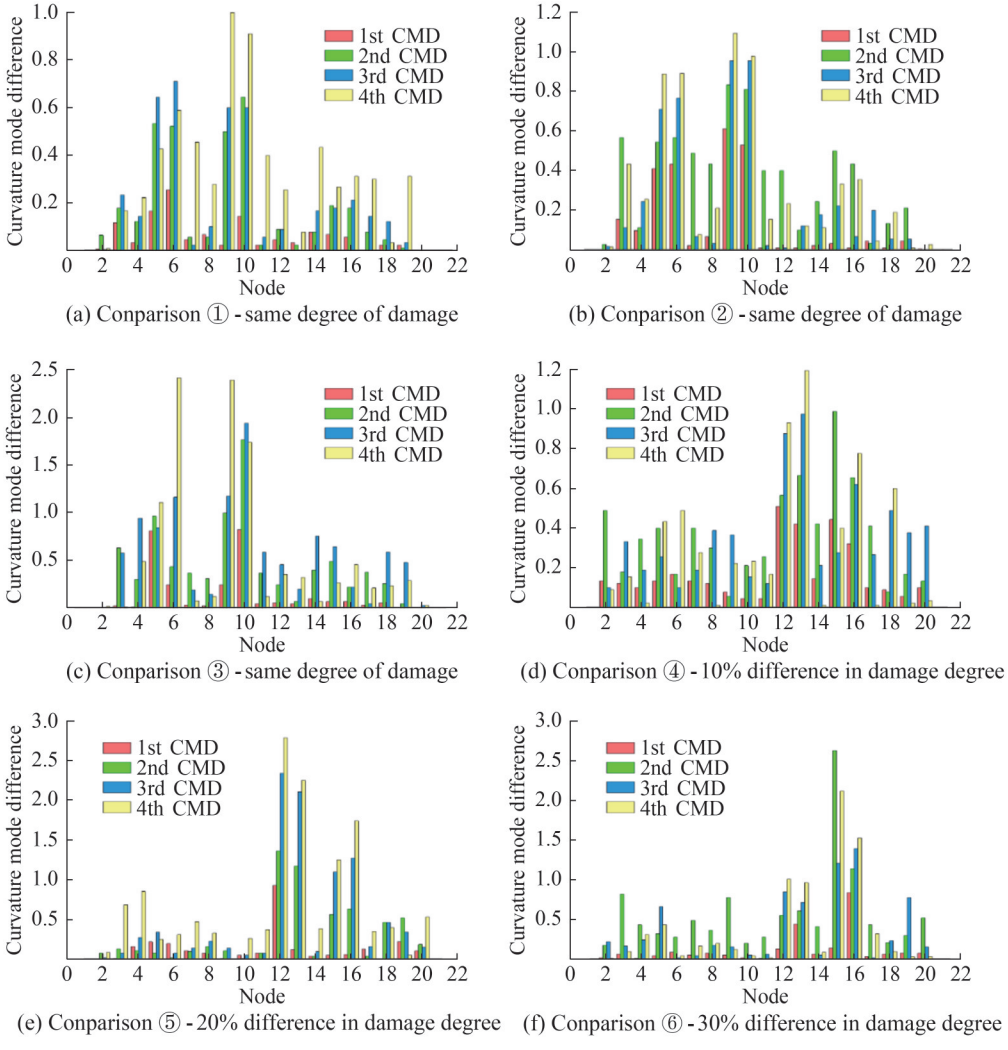


Figure 10 Curvature mode difference of the experiment for two simultaneous damage

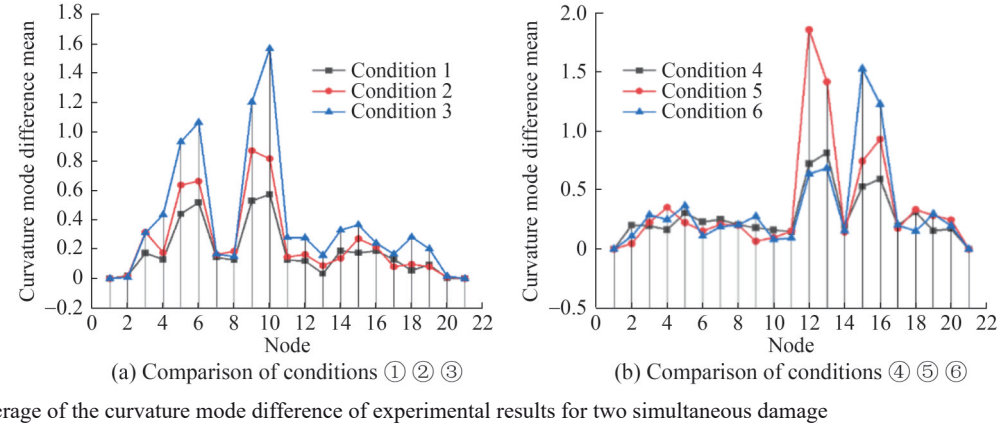


Figure 11 Average of the curvature mode difference of experimental results for two simultaneous damage

degree is small, the 1st order curvature mode difference is not much differentiated in unit 12 compared to the other units. It can be concluded that the 1st order curvature mode difference identification is less effective when the damage degree of the damaged unit is small.

The curvature mode differences for the first four modes are averaged and compared, with the results shown in Figure 13.

Figure 13 shows that when the ship sustains additional damage, the peak in the mean value of the curvature mode difference corresponds to the location of the second damage, accurately identifying the damaged unit. As the damage degree increases, the index at the damage location gradually

rises, demonstrating clear differentiation. The experimental results are shown below.

Figure 14 shows that for conditions ①, ②, and ③, the overall trend of curvature mode difference is the largest near unit 5. But there exist different interference peaks. In condition ①, only the 4th order curvature mode difference is clearly located in unit 5. In condition ②, only the 1st and 2nd order curvature mode differences can be ignored for the other interference peaks. In condition ③, only the 2nd and 4th order curvature mode differences interfere with the peaks to a lesser extent. The overall trend of the curvature mode difference of each order in conditions ④, ⑤ and ⑥

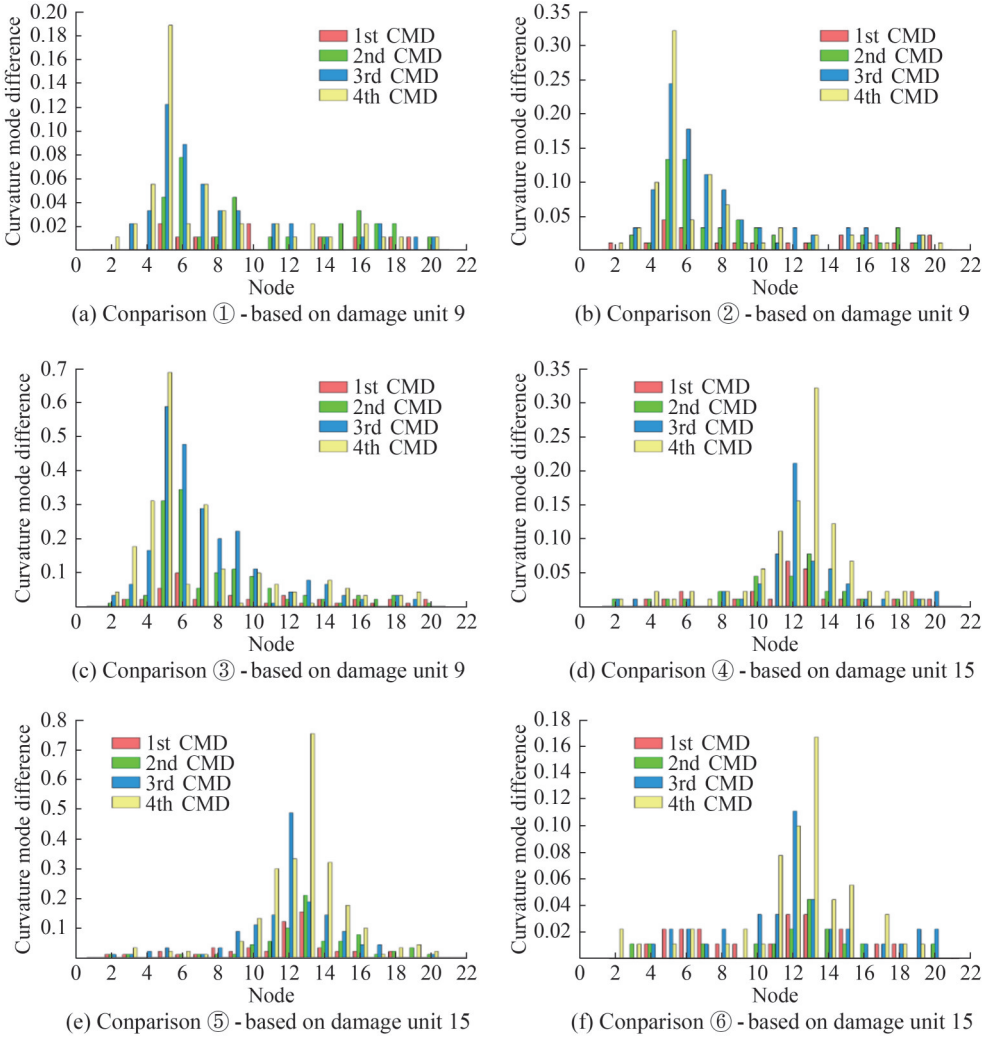


Figure 12 Simulation curvature mode difference for two damages that occur one after another

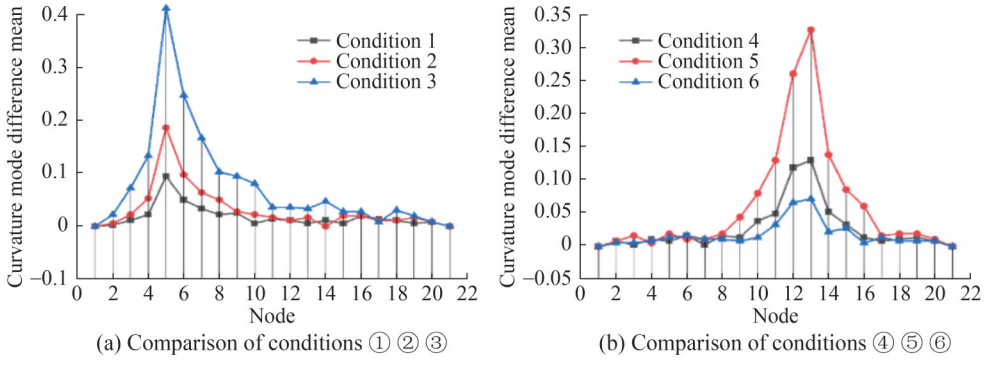


Figure 13 Average value of the curvature mode difference of simulation results for two damages that occur one after another

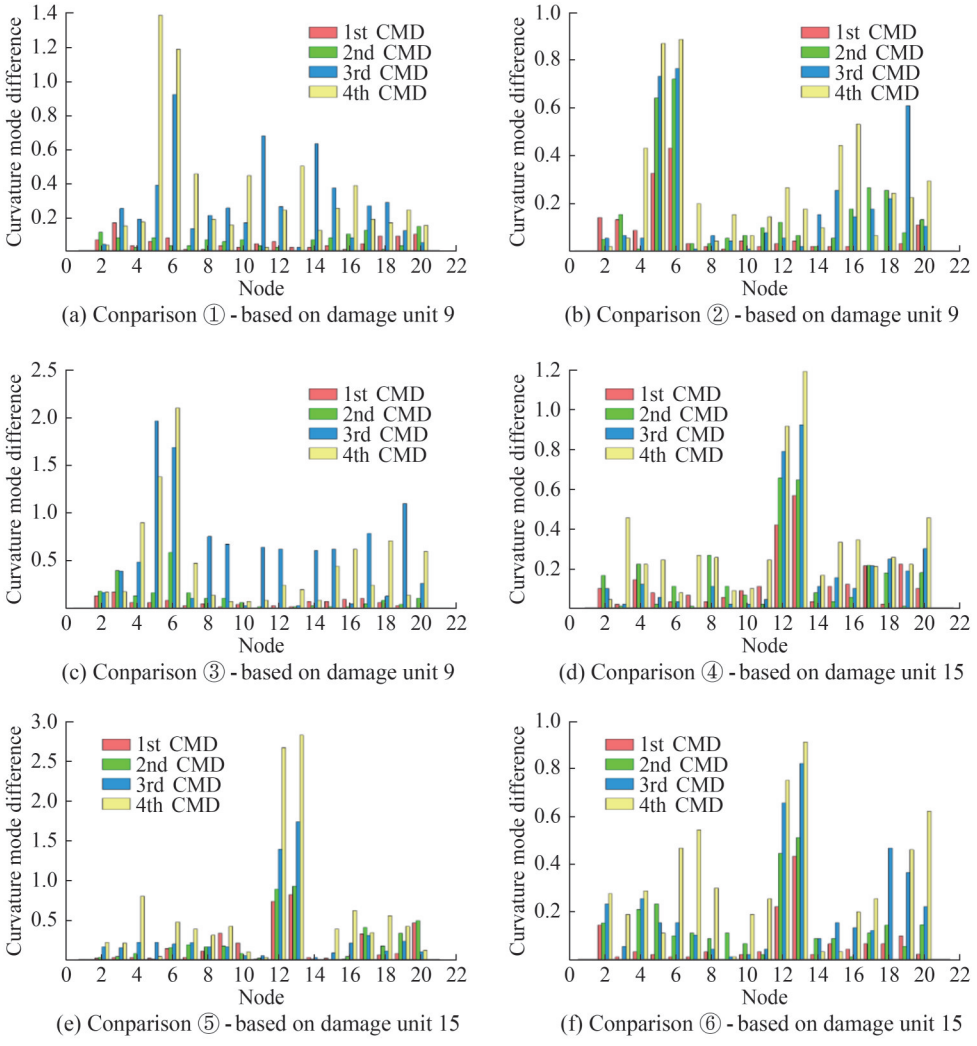


Figure 14 Curvature mode difference of the experiment for two damages that occur one after another

is maximum near unit 12. In condition ④, there exist interference peaks of all orders, but not to a large extent. In condition ⑤, the curvature mode differences are accurately located in unit 12. In condition ⑥, the 1st and 2nd order curvature mode differences are only the most obvious peak at unit 12. The 3rd and 4th order curvature mode differences are the largest at unit 12. But there are other interference peaks of different degrees. The degree of damage is negatively correlated with the peak of interference.

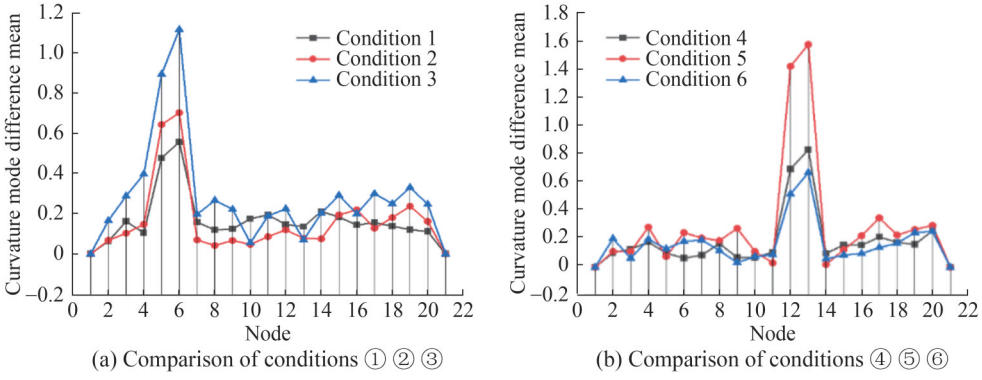
The mean values of the curvature mode differences for the same damaged unit at varying damage degrees in the experiment are compared, and the results are presented in Figure 15.

Figure 15 shows that when one damage already exists, the peaks of the average curvature mode differences across the first four modes correspond to the unit at the second damage location for all conditions, demonstrating accurate identification results. Although interference peaks of different degrees are observed in all conditions, their impact is minimal. As the damage degree increases, the mean curvature mode difference at the damage position gradually increases, showing a clear distinction.

When the ship sustains a second damage, the mean curvature mode difference index can accurately identify the location of this new damage without being affected by the existing damage. While each order of the curvature mode difference exhibits different degrees of interference peaks depending on the damage degrees, averaging the curvature mode difference notably reduces these interferences. The curvature mode difference index also shows a positive correlation with the damage degree, making it effective for assessing the damage degree.

4.3 Damage degree identification based on curvature mode difference

For ships, attacks often occur consecutively with time differences. Therefore, curvature mode differences obtained based on single damage conditions are used to identify the damage degree. The results are presented in Table 6.



(a) Comparison of conditions ① ② ③ (b) Comparison of conditions ④ ⑤ ⑥

Figure 15 Average of the curvature mode difference of experimental results for two damages that occur one after another

Table 6 Damage degree identification results

Condition	Pre-existing damage	Damage unit	Actual damage degree	Simulation identification		Experiment identification	
				Degree	Error	Degree	Error
①	Unit 9	Unit 5	15%	19.80%	32.00%	21.48%	43.20%
②			25%	38.15%	52.60%	42.95%	71.80%
③			45%	53.58%	19.06%	64.96%	44.36%
④	Unit 15	Unit 12	25%	20.33%	18.68%	21.91%	12.36%
⑤			45%	57.60%	28.00%	63.82%	41.82%
⑥			15%	13.55%	9.67%	19.99%	33.27%

Table 6 shows that the identification error for the damage degree in unit 12 is generally smaller than that in unit 5. The largest identification error for unit 5 reaches 25%. The error in damage identification results does not show a significant correlation with the actual damage degree. However, in the simulation, the error for unit 12 tends to increase as the actual damage intensifies. The simulation and experimental identification results show notable differences from the actual damage degree, with the experimental errors being generally larger. This phenomenon may be attributed to the high measurement accuracy and dense measurement point placement by curvature mode analysis. The experimental results are further affected by interference noise and discrepancies between the fitted vibration patterns and the actual vibration patterns of the model.

5 Conclusions

For ships, multiple successive attacks can seriously impact the structural safety of the hull. In this paper, different double damage conditions in hull girders are identified using the curvature mode index based on two cases of ship attacks. The main conclusions of the findings are as follows:

1) The test scheme optimization method proposed in this paper can rapidly determine the optimal modal information testing scheme for the beam model. The best evaluation index reaches 4.08, indicating that the obtained modal information is highly reliable and suitable for subsequent damage identification.

2) When two damages occur simultaneously, the mean curvature mode difference index can effectively identify the locations corresponding to the two damages. Furthermore, the index values are similar when the two damages have the same damage degree. When the ship sustains a subsequent attack, the mean curvature mode difference index can accurately locate the second damage without interference from the first damage, achieving a positioning accuracy of 100%.

3) The damage identification method based on the curvature mode proposed in this paper achieves 100% accuracy in locating damage positions. However, when quantitatively identifying double damages, the average error of damage degree estimation reaches 41.14%. This error is mainly attributed to noise interference. Therefore, one recommendation is to apply noise reduction techniques to the signals in practical applications to improve accuracy.

Competing interest The authors have no competing interests to declare that are relevant to the content of this article.

References

Ahmad S, Waleed A, Virk US, Riaz MT, Sharjeel A, Ahmad N (2019) Multiple damage detections in plate-like structures using

curvature mode shapes and gapped smoothing method. Adv. Mech. Eng. 11: 1687814019848921. https://doi.org/10.1177/16878140211016153

Altunisik AC, Okur FY, Kahya V (2017) Modal parameter identification and vibration based damage detection of a multiple cracked cantilever beam. Eng. Fail. Anal. 79: 154-170. https://doi.org/10.1016/j.engfailanal.2017.04.026

Cao M, Radzienski M, Xu W, Ostachowicz W (2014) Identification of multiple damage in beams based on robust curvature mode shapes. Mech. Syst. Signal Process. 46: 468-480. https://doi.org/10.1016/j.ymssp.2014.01.004

Cheng H, Guo J, Zhang Y, Li W (2023) Experimental research on damage identification of fully free beams based on modal shapes. Appl. Ocean Res. 139: 103689. https://doi.org/10.1016/j.apor.2023.103689

Hu M, Sun X, He J, Zhan Y (2019) Double crack damage identification of welded steel structure based on LAMB WAVES of S0 Mode. Materials 12(11): 1800. https://doi.org/10.3390/ma12111800

Janeliukstis R, Rucevskis S, Wesolowski M, Chate A (2017) Multiple damage identification in beam structure based on wavelet transform. Procedia Engineering 172: 426-432

Kuroki H, Kondou T, Bonkobara Y, Sakamoto Y (2011) Multiple damage identification analysis based on filtering theory for a framed structure by using low order natural frequency change. 14th Asia Pacific Vibration Conference (APVC) on Dynamics for Sustainable Engineering, 1493-1502

Le J, Lu L, Wang Y, Song H, Xing X, Huang C (2019) Damage identification of low-density material-filled sandwich panels with truss core based on vibration properties. Struct. Health Monit.- Int. J. 18: 1711-1721. https://doi.org/10.1177/1475921718820100

Ma Q, Solis M (2019) Multiple damage identification in beams from full-field digital photogrammetry. J. Eng. Mech. 145: 04019054. https://doi.org/10.1061/(ASCE)EM.1943-7889.0001629

Ouyang Q, Zhou L, Liu X (2016) Multiple damage identification and imaging in an aluminum plate using effective Lamb wave response automatic extraction technology. Conference on Sensors and Smart Structures Technologies for Civil, Mechanical, and Aerospace Systems, 98034J

Pandey AK, Biswas M, Samman MM (1991) Damage detection from changes in curvature mode shapes. J. Sound Vib. 145: 321-332. https://doi.org/10.1016/0022-460X(91)90595-B

Wu C, Liu H, Qin X, Tan G, Gu Z (2017) Multi-stage method to identify structural damage using multiple damage location assurance criterion and an improved differential evolution algorithm. Int. J. Comput. Intell. Syst. 10: 1066-1081. https://doi.org/10.2991/ijcis.2017.10.1.71

Xie F, Jiang Z, Jiang H (2018) A multi-damages identification method for cantilever beam based on mode shape curvatures and kriging surrogate model. 6th International Conference on Computer-Aided Design, Manufacturing, Modeling and Simulation (CDMMS), Busan, 030022

Yang Z, Chen X, Tian S, He Z (2012) Multiple damages detection in beam based approximate waveform capacity dimension. Struct. Eng. Mech. 41: 663-673

Zhang Y, Guo J, Hao N, Yang J, Li S (2020) Damage detection on hull girder of ship subjected to explosion loading. Ocean Eng. 198: 107006. https://doi.org/10.1016/j.oceaneng.2020.107006

Zhang Y, Guo J, Jia T, Cheng H (2022a) Experimental research on frequency based damage identification of beams with free boundary condition. Ocean Eng. 266: 112901. https://doi.org/10.1016/j.oceaneng.2022.112901

Zhang Y, Guo J, Xie Y, Xu J (2022b) Warship damage identification using mode curvature shapes method. Appl. Ocean Res. 129: 103396. https://doi.org/10.1016/j.apor.2022.103396

Zhang Y, Guo J, Xu J, Li S, Yang J (2021a) Study on the unequivalence between stiffness loss and strength loss of damaged hull girder. Ocean Eng. 229: 108986. https://doi.org/10.1016/j.oceaneng.2021.108986

Zhang Y, Guo J, Zhou Q, Wang S (2021b) Research on damage identification of hull girder based on Probabilistic Neural Network (PNN). Ocean Eng. 238: 109737. https://doi.org/10.1016/j.oceaneng.2021.109737